JOURNAL OF THE CANADIAN SOCIETY OF EXPLORATION GEOPHYSICISTS
VOL. 23, NO. 1 (DEC. 1987), P. 27-36

AMPLITUDE-VS-OFFSET ANALYSIS: A REVIEW WITH REFERENCE TO APPLICATION IN WESTERN CANADA[1]

SUDHIR JAIN[2]

ABSTRACT

It is well known that P- and S-wave velocities (V_p, V_s) taken together are better indicators of lithology and fluid content than P-wave velocities alone. Offset-amplitude studies from CDP gathers have been proposed as a method of determining S-wave velocities from P-wave recordings. The Knott-Zoeppritz equations relate amplitude of a reflection from an acoustic discontinuity to V_p, V_s and the angle of incidence. Therefore, in theory, it is possible to use CDP gathers to determine V_p from normal moveout and V_s from amplitudes. Moreover, it has been noted that as incidence approaches the critical angle, amplitude and phase of the reflected wave show sudden increases and that, with certain combinations of V_p and V_s, polarity reversal is possible at certain angles of incidence.

The paper discusses these characteristics in detail with reference to situations of practical exploration interest in western Canada. While the transparent reflectors can be expected to become prominent at narrow incidence angles, the model studies show that for translucent Cretaceous gas prospects in central Alberta and for recording spreads of practical dimensions, the phase of reflected waves is stable and amplitude changes on CDP gathers are too small to be reliably mapped in the presence of noise due to surface waves and other sources.

INTRODUCTION

Pickett (1963) found from laboratory measurements that the ratio of compressional-wave velocity (V_p) and shear-wave velocity (V_s) is diagnostic of the rock type. Tatham (1982) reviewed the published work on V_p and V_s and concluded that V_p/V_s has an association with lithology as well as porosity, aspect ratio and fluid content. An extensive sonic-log library is available concerning V_p. However, logging for V_s is quite rare and the information regarding in-situ S-wave velocities is scarce. Amplitude-vs-offset (AVO) studies have been proposed (Ostrander, 1984) as a method of using reflection amplitudes on CDP gathers to obtain V_p/V_s or Poisson's ratio at little extra cost.

Zoeppritz's equations (Young and Braile, 1976) relate the amplitude and phase of transmitted and reflected P- and S-waves to incident P-wave amplitude, P- and S-wave velocities and densities on both sides of the reflector. Therefore, the CDP gathers can be used to compute P-wave velocity (V_p) from normal moveout and S-wave velocity (V_s) from amplitudes. Densities can be estimated using empirical relationships such as that given by Gardner *et al.* (1974). Inconsistencies between V_p and V_s are indicated conveniently by Poisson's ratio, P, which is related to V_p and V_s by the simple equation:

$$V_p/V_s = [(1 - P)/(0.5 - P)]^{1/2}$$

This paper reviews available publications on V_p and V_s to estimate parameters applicable in the western Canadian basin. Several aspects of Zoeppritz's equations are discussed and model studies are described which indicate that the variations due to lithology and fluid content in translucent Cretaceous reservoirs of central Alberta are not likely to be mappable from amplitude analysis of prestack data.

V_p, V_s AND P VS LITHOLOGIC PARAMETERS

V_p can be accurately determined from sonic logs in known areas and by inversion processing of seismic data in unknown areas. However, S-wave logging is not common and shear-wave velocity data come either from theoretical studies (Kuster and Toksöz, 1974) or from laboratory studies of rock samples (Pickett, 1963; Domenico, 1974, 1976, 1984; Gregory, 1976; Toksöz *et al.*, 1976; Wilkens *et al.*, 1984; Castagna *et al.*, 1985, Han *et al.*, 1986). There is a fair degree of general agreement on V_p and V_s for sedimentary rocks and P values can be estimated within a fairly narrow range. There appears to be no published work dealing with V_p/V_s in the western Canadian basin and specific values can only be estimated from studies in other areas.

Kuster and Toksöz (1974) give detailed equations relating porosity, aspect ratio (ratio of minimum dimension to maximum dimension of the pore) and elastic properties to V_p and V_s in a completely impermeable

[1]Presented at the C.S.E.G. National Convention, Calgary, Alberta, May 13, 1987. Manuscript received by the Editor June 5, 1987; revised manuscript received October 9, 1987.

[2]Commonwealth Geophysical Development Co. Ltd., 1701, 505 - 3 Street S.W., Calgary, Alberta T2P 3E6

rock. In spite of this constraint, general conclusions derived from their equations are supported by laboratory studies. Figures 1 and 2 show calculated P-wave velocity and Poisson's ratio respectively for water- and gas-saturated sandstones and limestones of porosity 0 to 10% and aspect ratio .03 to .14. In water-filled sandstone P shows a slight increase, while in gas-filled sandstone P declines rapidly with increasing porosity. In limestones, P declines with increasing porosity, more rapidly when gas-filled. The absolute value of P depends on elastic properties of the rocks. Sandstone values in Figure 1 are a little lower than laboratory studies show, while limestone values in Figure 2 are a little higher. Both figures show that shape of the pores is an important determinant for P.

Laboratory studies on unconsolidated sands by Domenico (1974, 1976) show that the presence of gas reduces V_p by as much as 30%, while V_s is marginally increased. This causes a dramatic drop in P in unconsolidated sands from 0.4 to 0.1. With increasing pressure, P decreases from 0.46 at atmospheric pressure (101 kPa) to 0.38 at 34 300 kPa in saturated sand. P values in water-filled sand are higher than can be expected in practice because of the difference in consolidation and clay content. Domenico (1984) gives the general range of P for sandstones to be from 0.17 to 0.26, for dolo-

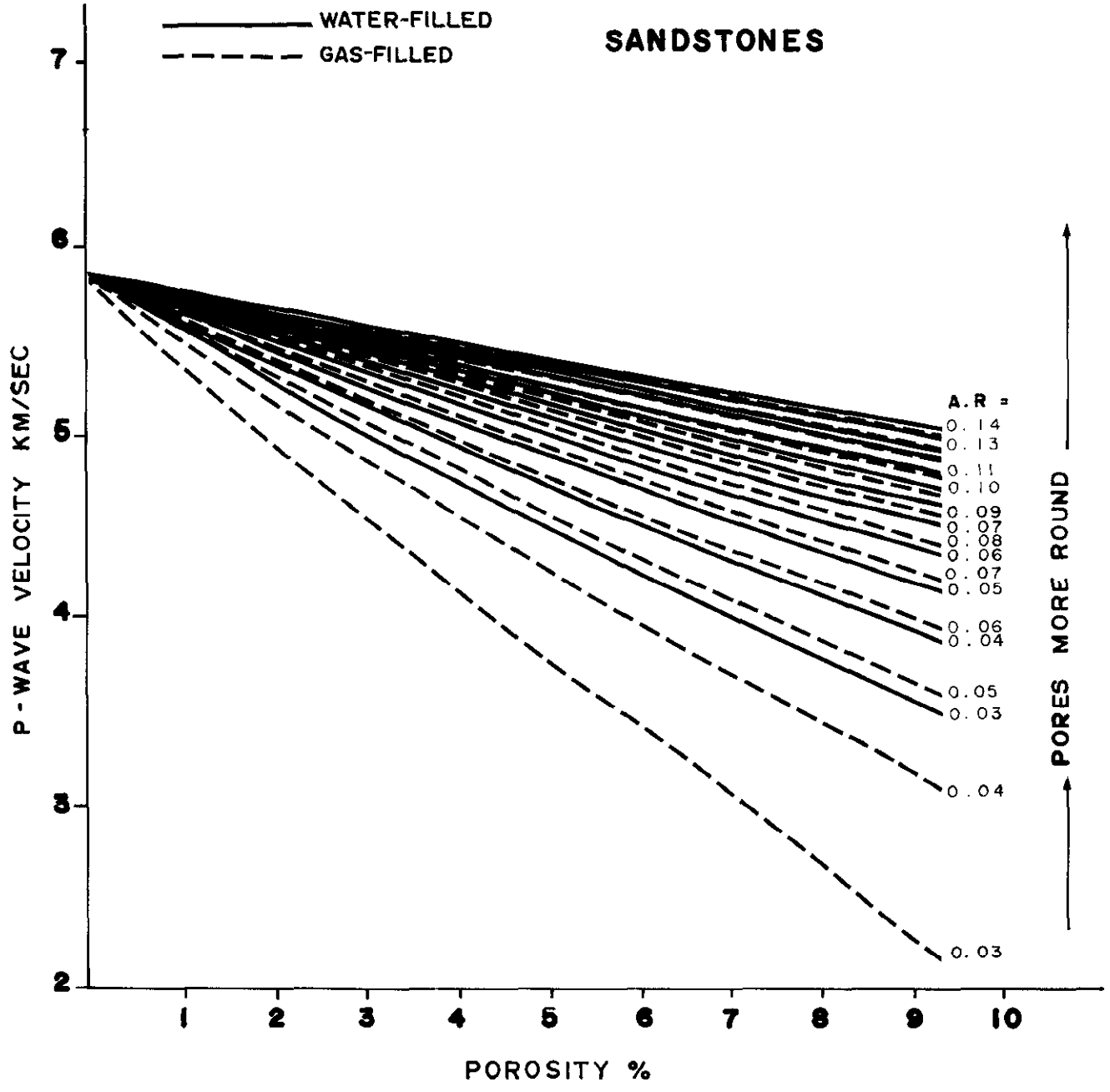

Fig. 1. a) Velocity of primary waves vs porosity for water- and gas-filled sandstones of variable pore shape.

mites from 0.27 to 0.29 and for limestones from 0.29 to 0.33. Gregory (1976) finds from sample studies that P increases by about 10% in highly porous water-filled rocks.

In gas-saturated sandstone P is considerably less, *i.e.*, 0.14 to 0.17 as compared with 0.20 to 0.30 in water-filled sandstones. Han *et al.* (1986) find that clay content is also an important parameter in determination of V_p, V_s and P. They derive the following empirical equations for water-filled sandstones:

$$V_p = 5.59 - 6.93\phi - 2.18C$$
$$V_s = 3.52 - 4.91\phi - 1.89C$$

where ϕ and C are fractional porosity and clay content respectively and V_p and V_s are in km/s. These equations show that both V_p and V_s decline with increasing porosity, as well as with increasing clay content. P increases with porosity as well as clay content. Han *et al.* (1986) find that partially saturated samples show much greater scatter and V_p is consistently lower. It is important to note that Domenico (1974, 1976) and Gregory (1976) find that the first 10% unsaturation (gas content) causes the most reduction in V_p.

Castagna *et al.* (1985) show that the trend line in V_p vs V_s for mudrock (shale) is the same as for the sandstones. They give slightly different empirical equa-

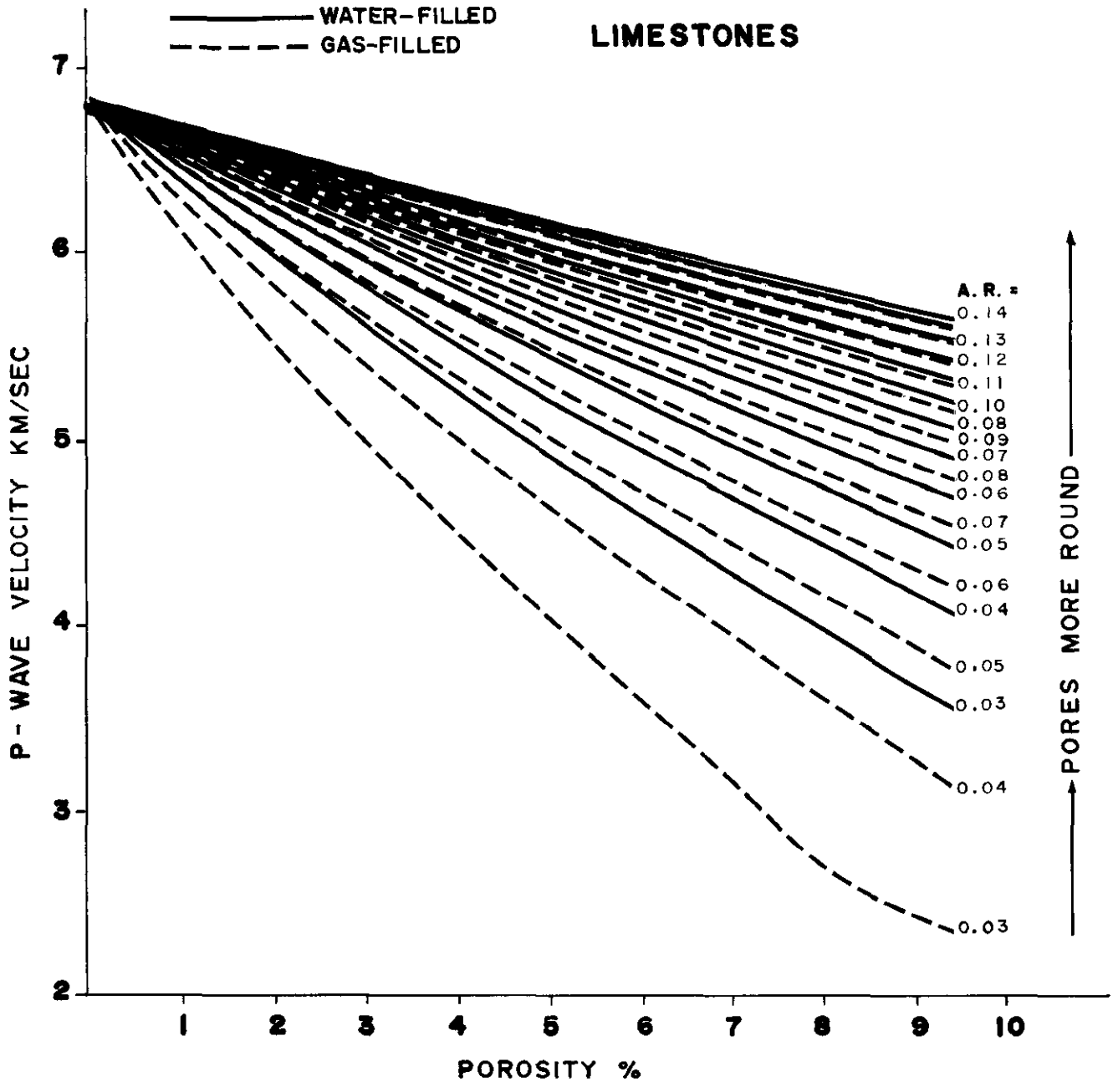

Fig. 1. b) Velocity of primary waves vs porosity for water- and gas-filled limestones of variable pore shape. The equations of Kuster and Toksöz (1974) were used.

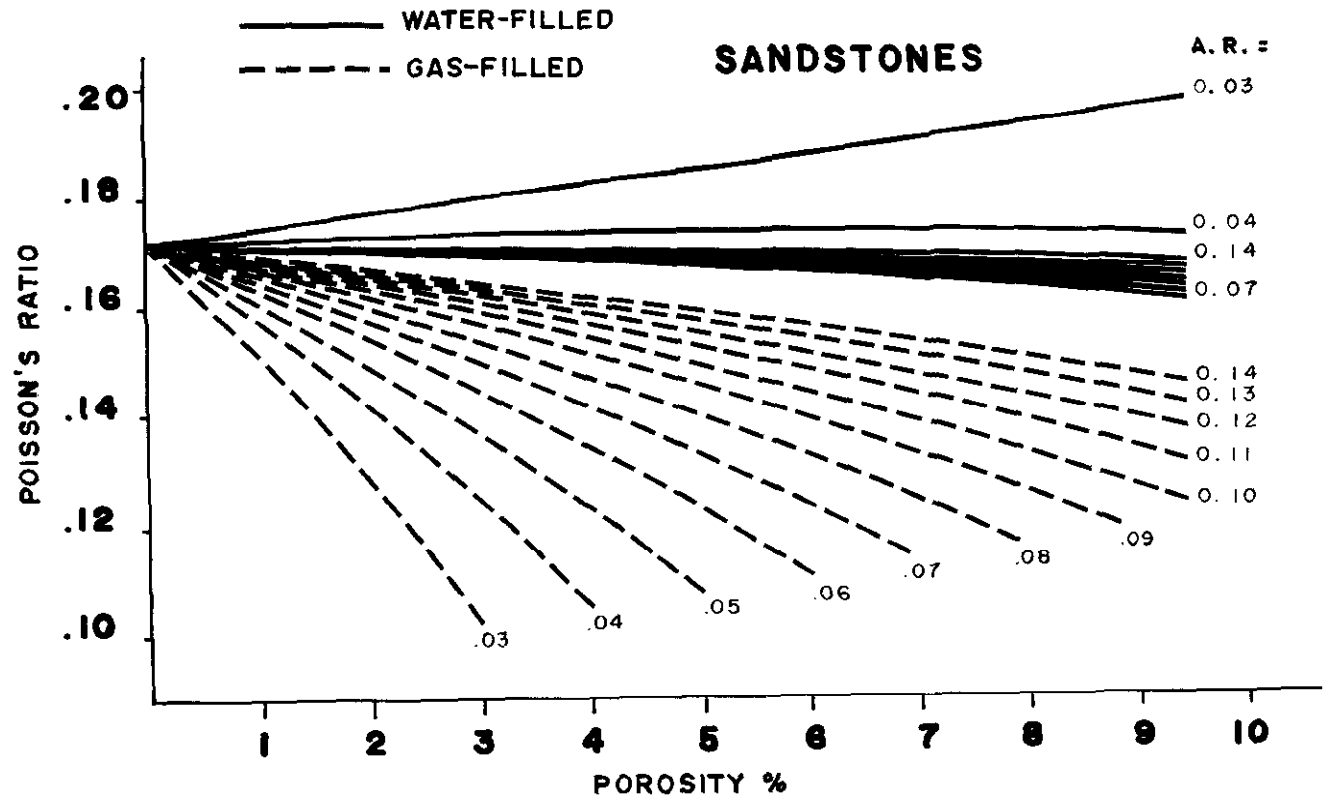

Fig. 2. a) *P* vs porosity for water- and gas-filled sandstones of variable pore shape.

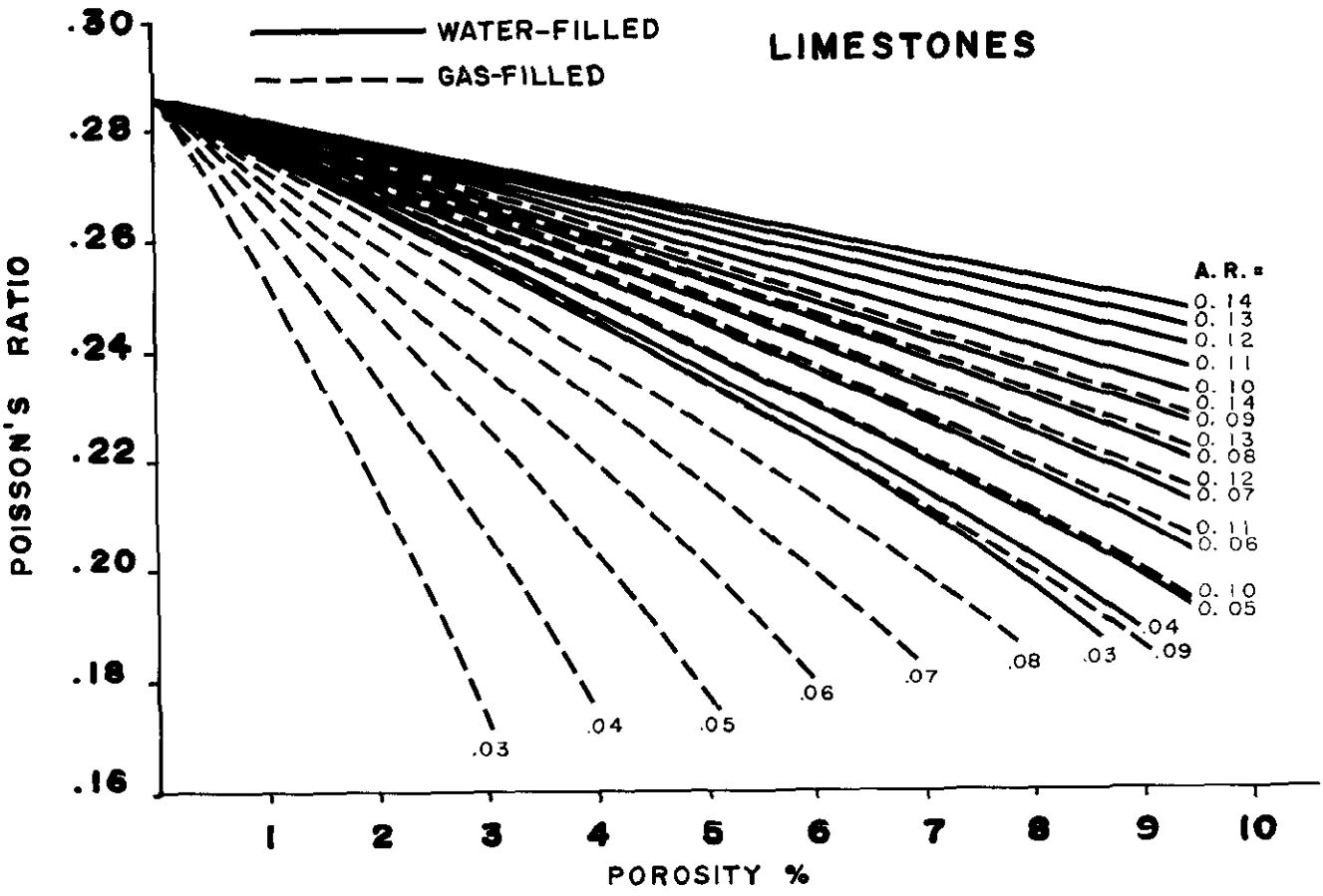

Fig. 2. b) *P* vs porosity for water- and gas-filled limestones of variable pore shape. The equations of Kuster and Toksöz (1974) were used.

tions for V_p and V_s, porosity and clay content, than Han *et al.* (1986), but the general trends are quite similar in both studies. For dry sandstones, the published studies converge on V_p/V_s of 1.5 ($P = 0.1$). In wet sandstones, there is an almost linear relationship between V_p and P, P declining from 0.5 for $V_p = 1.4$ km/s to 0.1 for $V_p = 5.8$ km/s. They also find that V_p/V_s is about 10% higher for noncalcareous than clean sands in Gulf Coast data.

In summary, theoretical and laboratory studies show a general consensus on the range of values for P in a variety of rock material. If V_p is known, P can be estimated with sufficient accuracy for model studies from a synthetic log. Generally, a dramatic decline in Poisson's ratio in a sand environment indicates the presence of gas though not the absence of oil. In sandstones, a small increase in P could indicate an increase in porosity or gradation into shales. In carbonates, a small decrease could indicate dolomitization or an increase in porosity. It is important to remember that the mineral content is at least as important as porosity in determination of P, particularly when small changes are involved.

Factors in Offset Amplitude Studies

Significance of curved raypath

The amplitude of a reflected wave relative to the incident wave is a function of angle of incidence, which depends on the depth Z, source-receiver distance X and the variation of velocity with depth. If the velocity down to the reflector is constant, the angle of incidence is simply $\tan^{-1}(X/2Z)$. However, if the velocity varies with depth, the raypath is no longer straight. Curvature of raypath depends on the velocity-depth relationship. In general terms, the velocity increases with depth, but this rate of increase depends on depth and lithology. Most logs in the western Canadian basin justify a linear increase in velocity with depth down to the Paleozoic unconformity. The incidence angle Θ_i at any depth can be computed for the relationship $V = V_o + KZ$ where K is the increase in velocity per kilometre of depth Z from the equation (Ostrander, 1984):

$$\Theta_i = \tan^{-1}\left(\frac{ZX + V_o X/K}{Z^2 + 2V_o Z/K - X^2/4}\right)$$

Inspection of sonic logs from western Canada shows that K ranges from 0.25 to 1.0 in the Cretaceous section. Elementary calculations show that for these values of K, the curved path does not diverge significantly from a straight raypath for incidence angles of less than 30°, which would include a source-receiver distance of 1.7 km and a 1.5 km deep reflector.

X/Z values given in subsequent figures have been computed using straight raypaths. The corrections required will be small for incidence angles of 30° or less. Even for larger angles, the given values are useful approximations.

Amplitude and phase near the critical angle

Young and Braile (1976) programmed Zoeppritz's equations to compute amplitude and phase of reflected and transmitted energy. Phase of the reflected energy is the same as incident energy for incidence angles less than the critical angle. For incidence larger than critical angle, phase angle increases dramatically and reaches 180° for grazing incidence. Where $V_{p2} < V_{p1}$, there is no critical reflection and the phase difference between reflected and incident energy is 180° for all incidence angles. On the other hand, the amplitude of the reflected wave is related to the angle of incidence even at near-normal incidence. Figure 3 is the plot of the reflected-wave amplitude vs angle of incidence for six different cases. This figure shows that the reflected-wave energy declines steadily until near-critical incidence is reached, at which point it increases dramatically.

Figure 4 is a nomogram showing vertical two-way traveltime vs critical distance for various ratios of V_1/V_2 and $V_1 = 3.0$ km/s. This is a good representation of velocity in Alberta for the Cretaceous section. For a vertical two-way time of 0.4 s this distance is 1.01 km for $V_1/V_2 = 0.4$ and 5 km for $V_1/V_2 = 0.9$. For 1.0 s the critical distance is 2.6 km at $V_1/V_2 = 0.4$ and 5.9 km at $V_1/V_2 = 0.7$. It is evident that the recording spread has to be extraordinarily long relative to depth to observe reflections in critical-angle zones. An exception is an anomalously high-velocity layer, like a basalt layer in a sand-shale sequence. A high-velocity intermediate layer refracts the wave very sharply on its way down and up and a high incidence angle is attained for the reflection from the base which can be received with source-receiver configurations generally used in western Canada.

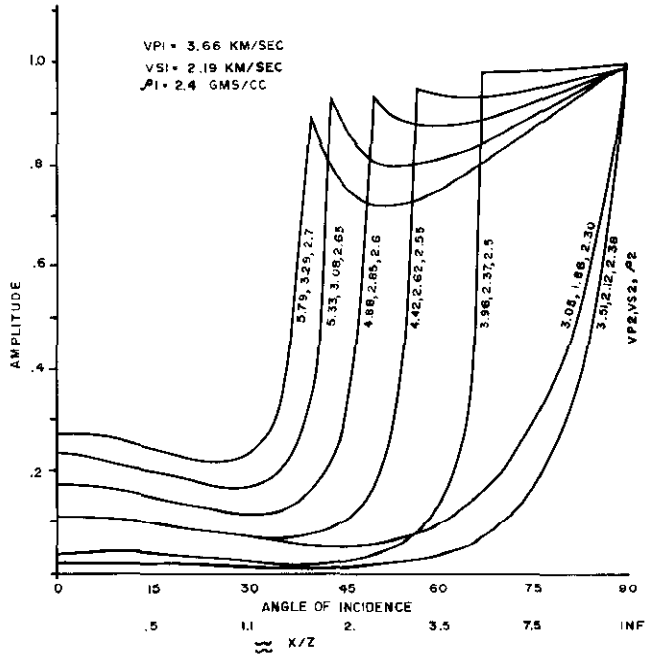

Fig. 3. Amplitude of reflected wave vs angle of incidence for seven two-layer models. Note the general decline up to critical angle and then sudden burst in reflected wave amplitude.

Shuey's simplification of Zoeppritz's equations

Shuey (1985) gives a simplified version of Zoeppritz's equations which is valid for angles up to critical incidence and is a fair representation of amplitudes even at larger angles of incidence. Shuey's approximation of Zoeppritz's equations is:

$$R(\Theta)/R_o \simeq 1 + A \sin^2\Theta + B(\tan^2\Theta - \sin^2\Theta) \quad (1)$$

where $R(\Theta)$ and R_o are the reflectivity coefficients for incidence angle Θ and for normal incidence respectively. A and B are described as follows:

$$B = (\Delta V_p/V_p)/(\Delta V_p/V_p + \Delta\rho/\rho)$$
$$A = B - 2(1+B)(1-2P)/(1-P) + \Delta P/(R_o(1-P)^2)$$

where ΔV_p, $\Delta\rho$ and ΔP are changes in P-wave velocity, density and Poisson's ratio across the interface and V_p, ρ and P are averages of P-wave velocities, densities and Poisson's ratio on the two sides. The numerator in B relates to P-wave velocity and the denominator to acoustic impedance. Allowing for uncertainties in generally accepted velocity-density relationships, B is expected to range from 0.7 to 0.9 for sedimentary rocks. In particular, if the empirical density-velocity relationship for different brine-saturated rock types, $\rho = 0.23\ V_p^{.25}$ (Gardner, *et al.*, 1974) is applied, $\Delta\rho / \Delta V_p = 0.25\ \rho/V_p$ and $B = 0.8$. In this case the behavior of $R(\Theta)/R_o$ is controlled mainly by A which can be written as

$$A = 0.8 - 3.6(1-2P)/(1-P) + \Delta P/(R_o(1-P)^2)$$

or

$$A = K_1 + K_2\,\Delta P/R_o \quad (2)$$

where

$$K_1 = -2.8 + 3.6P/(1-P),\ K_2 = 1/(1-P)^2,$$

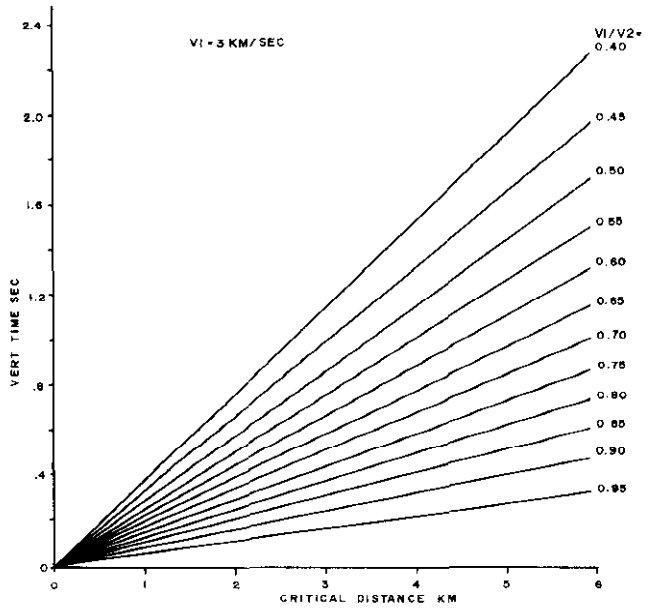

Fig. 4. Nomogram showing vertical two-way time vs critical distance of various ratios of V_p across the reflector.

substituting

$$R_o \approx (\Delta V_p/V_p + \Delta\rho/\rho)/2 \approx 0.625\,\Delta V_p/V_p$$
$$A \approx K_1 + K_{22}\,V_p\,\Delta P/\Delta V_p$$

where $K_{22} = 1.6/(1-P)^2$. (3)

Since K_1 is negative for all practical values of P and K_2 is generally smaller in magnitude than K_1, equation (2) explains why amplitudes in Figure 3 decline with increasing angle of incidence until Θ becomes greater than 30° when the third term in equation (1) becomes larger than the second term. Note that in the case of an acoustically transparent reflector, R_o is very small and if ΔP is significant, small changes in acoustic impedance cause significant changes in $\Delta P/R_o$ and therefore in A. This will cause significant changes in $R(\Theta)/R_o$ which may or may not be associated with changes in ΔP. In this way, amplitude-offset analysis can be used to identify anomalies in near-transparent reflectors even though the causes of anomalies cannot be unambiguously determined from amplitudes alone. One such case is discussed by Varsek *et al.* (1987). Note that K_1 and K_2 are determined by the average value of P across the reflector, and changes in A (therefore $R(\Theta)/R_o$ at near-normal incidence) are governed largely by changes in $\Delta P/\Delta V_p$, not ΔP alone as is sometimes believed.

Estimation of $\Delta P/\Delta V_p$

To get some idea of the expected ralationship between V_p and P, P and V_p, values in Figures 1 and 2 were expanded for a greater variety of elastic moduli and P vs V_p plotted for brine- or gas-filled sandstones and limestones (Figures 5 to 8). Generally, there is a direct relationship between P and V_p. Equation (3) shows that, if the relationship were linear, A would be constant. However, the P vs V_p relationship is not quite linear and some changes in A are expected with change in P or V_p. The magnitude of these changes depends on the

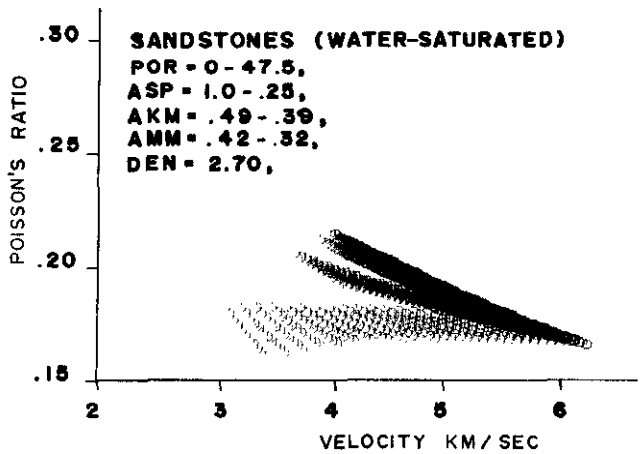

Fig. 5. Poisson's ratio vs V_p for water-saturated sandstones using the equation by Kuster and Toksöz (1974). In this and the following three figures, AKM = bulk modulus, AMM = shear modulus, ASP = aspect ratio, POR = porosity in percent and DEN = density of the rock sample in g/cm^3.

curvature in the P vs V_p relationship. It should be pointed out that the P vs V_p relationship in any particular case is not represented by the median or any other line through the points because the elastic properties do not necessarily correspond to those of the median points.

Polarity reversal with offset

Wren (1984) suggests the possibility of observing polarity reversals with increasing offset. Phases of reflected and incident waves are identical until critical incidence (Tooley *et al.*, 1965). Phase rotation begins at this point and reaches $\pi/2$ at grazing incidence. Polarity reversal at less than critical incidence can occur only if $R(\Theta)/R_o$ becomes negative. For this to happen, A in equation (2) or (3) must be less than -4 for $\Theta = 30°$. If $P = 0.2$, then $K_1 = -1.9$, $K_2 = 1.56$ and $K_{22} \approx 2.5$. Large negative values of A are possible when $\Delta P/R_o$ is less than -1.34 ($V_p\ \Delta P/\ \Delta V_p$ less than -0.8). For translucent interfaces ($R_o = 0$) this can only occur if P decreases significantly while velocity increases only slightly, as indeed is the case in Figure 2 of Wren (1984). In view of studies discussed above and as pointed out by Shuey (1985) this is not likely to occur often in practice. On the other hand when $R_o \approx 0$, small negative values of P can cause sufficiently large negative values of A and polarity reversals in $R(\Theta)$. Therefore, large offset-amplitude changes at near-normal incidence coupled with polarity reversal indicate change in the opposite direction of P and V at a near-transparent interface.

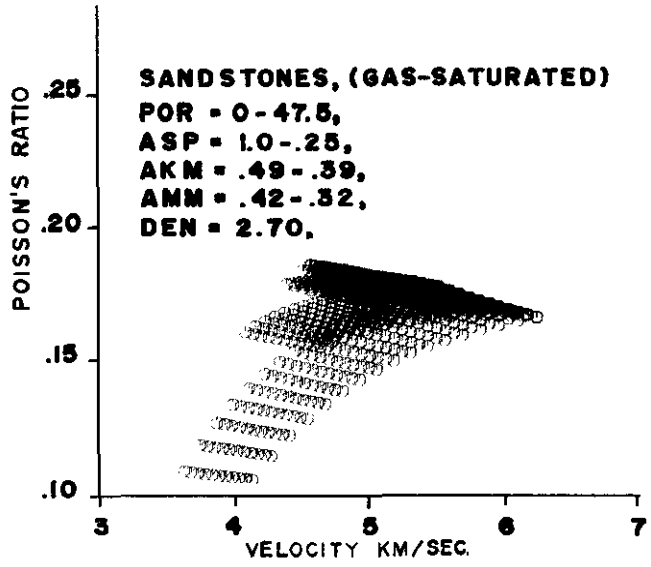

Fig. 6. Poisson's ratio vs V_p for gas-filled sandstones using the equation of Kuster and Toksöz (1974).

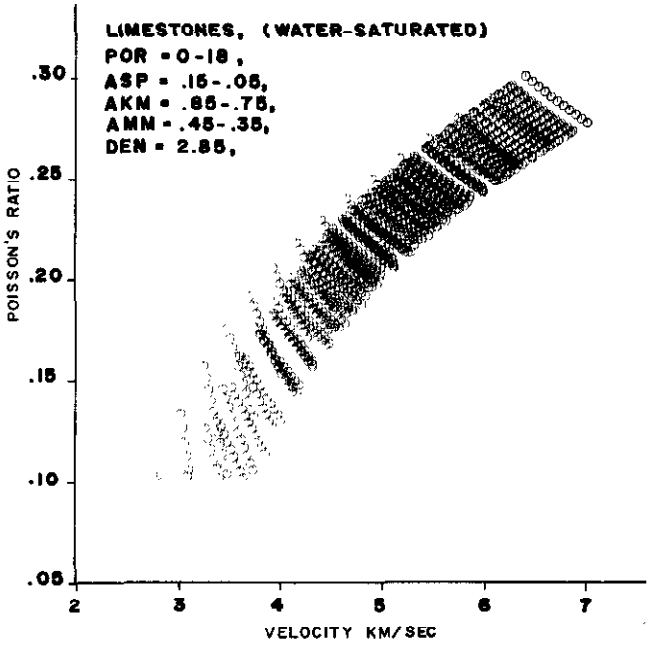

Fig. 7. Poisson's ratio vs V_p for water-saturated limestones using the equation of Kuster and Toksöz (1974).

$R(\Theta)/R_o$ vs Θ and A for typical sand beds

Equation (1) was used to plot a set of curves (Figure 9) which are quite revealing. The curves were computed for the velocity of 2.75 km/s at the surface and 4.0 km/s at the reflector located at the depth of 1.5 km, which corresponds to many typical sand plays in central Alberta. $R(\Theta)/R_o$ is plotted against source-receiver distance and the corresponding angle of incidence for a linear increase of velocity with depth. A ranges from -2 to 1 which covers the range of $V_p\ \Delta P/\Delta V_p$ from 0 to 1.2.

Figure 9 shows the amplitude ratio for spread distance up to 3.0 km (incidence angle up to 71°). The curve for $A = 0$ shows the contribution to amplitude increase by the third term, $B(\tan^2\Theta - \sin^2\Theta)$. This

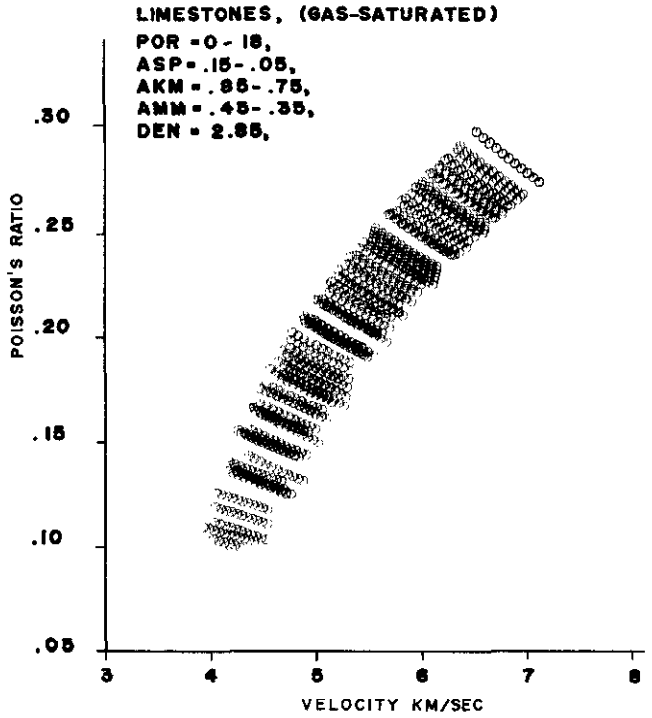

Fig. 8. Poisson's ratio vs V_p for gas-filled limestones using the equation of Kuster and Toksöz (1974).

curve shows that this term becomes significant at Θ = 30° and dominates $R(\Theta)/R_0$ beyond Θ = 45°.

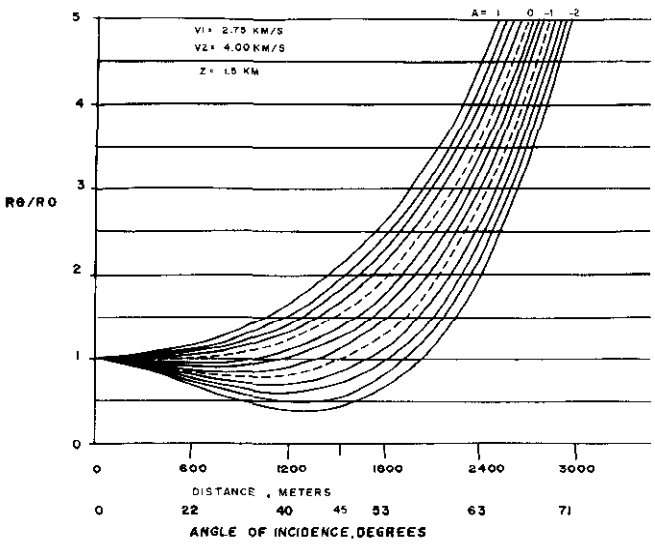

Fig. 9. $R(\Theta)/R_0$ vs angle of incidence or offset for a reflector located at 1.5 km. The $A = 0$ curve indicates the contribution of the third term on the right in equation (1).

This increase in amplitude beyond Θ = 45° can be used to compute Θ, and therefore P-wave velocity. However, considering possible errors in estimating amplitude ratios on real data, one can expect deviations in estimated Θ which will cause errors in velocity computation comparable to those from normal moveout and make the extra expense of larger spreads unjustified. Note that a change of 0.3 in A (0.1 in V_p $\Delta P/\Delta V_p$) causes a change in amplitude of the farthest trace of about 15%. This is usually within the noise envelope and lithologic changes in reservoir properties can be delineated in offset amplitudes only in noise-free data. If larger changes were expected in A (*i.e.* V_p $\Delta P/\Delta V_p$) indicative of strong anomalies in V_p and/or P, then amplitude anomalies on the farther traces would be more significant.

Thin-layer model

The effect of changes in V_p and P in the thin-reservoir case can be estimated by integrating the response of all the reflectors in a section of appropriate length around the reservoir. Figures 10 and 11 show two of the numerous models studied by the author and produced using

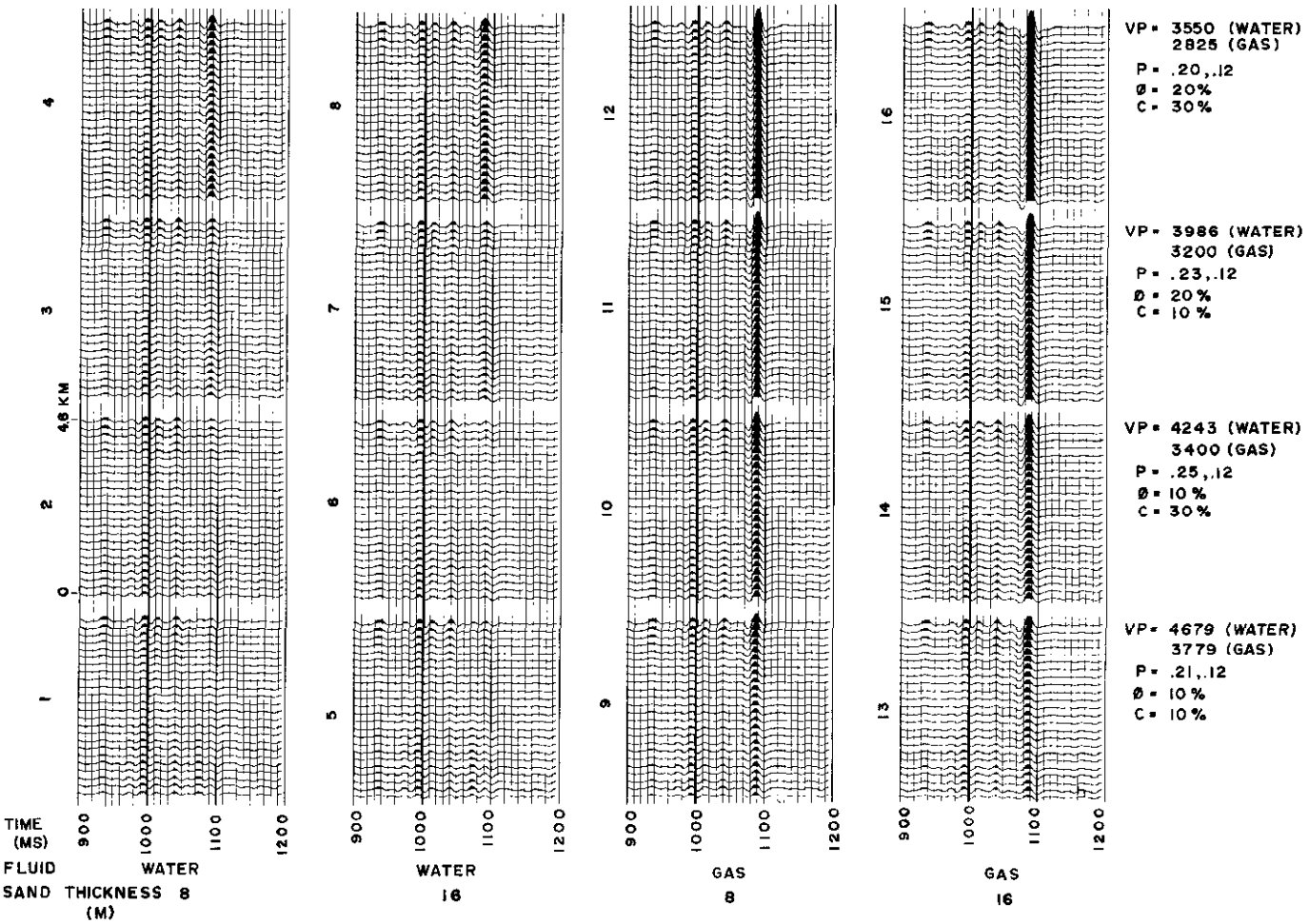

Fig. 10. Synthetic response for sands of thickness 8 and 16 ms for various possible values of V_p and P. Values of porosity (ϕ) and clay content C on the right correspond to all sections in that row. Values of V_p and Poisson's ratio (P) correspond respectively to water- or gas-bearing sand in the row.

Zoeppritz's equations. In each model, V_p is changed in sand zones of thickness 4 ms (8 m) and 8 ms (16 m) occurring in a sand-shale environment at 1.084 s. Porosity and clay content in the sand range from 10 to 30%. V_p and V_s were computed according to the generalized equation given by Han *et al.* (1986). A zero-phase wavelet (12/18 70/90 Hz) was used. In Figure 10, P changes with any change in porosity or clay content while in Figure 11, P is held constant at 0.24. A comparison of the two figures shows that significant changes in P cause only small differences in relative offset-amplitudes and those only at offsets of approximately 4000 m — almost twice the depth. Figure 12 shows the amplitude coefficient A computed from amplitudes in Figure 10 using actual sonic velocities to compute respective Θ values. Trace numbers correspond to those of the source models in Figure 10. Amplitude coefficients from the first twelve traces (maximum offset 2.2 km) are shown at the top and those from all traces at the bottom. Even when the parameters are perfectly known, computed amplitude coefficients from the 2.2 km spread are unchanged for all models. Amplitude coefficients from all traces show small changes at 1.08 s which can probably be observed in real data only when noise of any kind is totally absent on unstacked data. This, unfortunately, is not the case in data recorded in western Canada.

Conclusion

The theoretical and laboratory studies in a variety of environments, indicate that V_p/V_s or P are related to porosity, aspect ratio, mineral content and liquid or gas content. In theory, it is possible to estimate P from amplitudes in CDP gathers. Amplitude increase and phase rotation beyond the critical angle can be observed if the spreads are two or more times as long as the depth. Amplitude anomalies at less than critical incidence can be observed in reflections from interfaces transparent at normal incidence across which there is significant change in Poisson's ratio. For nontransparent interfaces with the recording configurations normally used in western Canada one can observe declining amplitude with increasing offset which is dependent on P. However, model studies show that the expected anomalies in these amplitude changes are very small even for unusually long spreads.

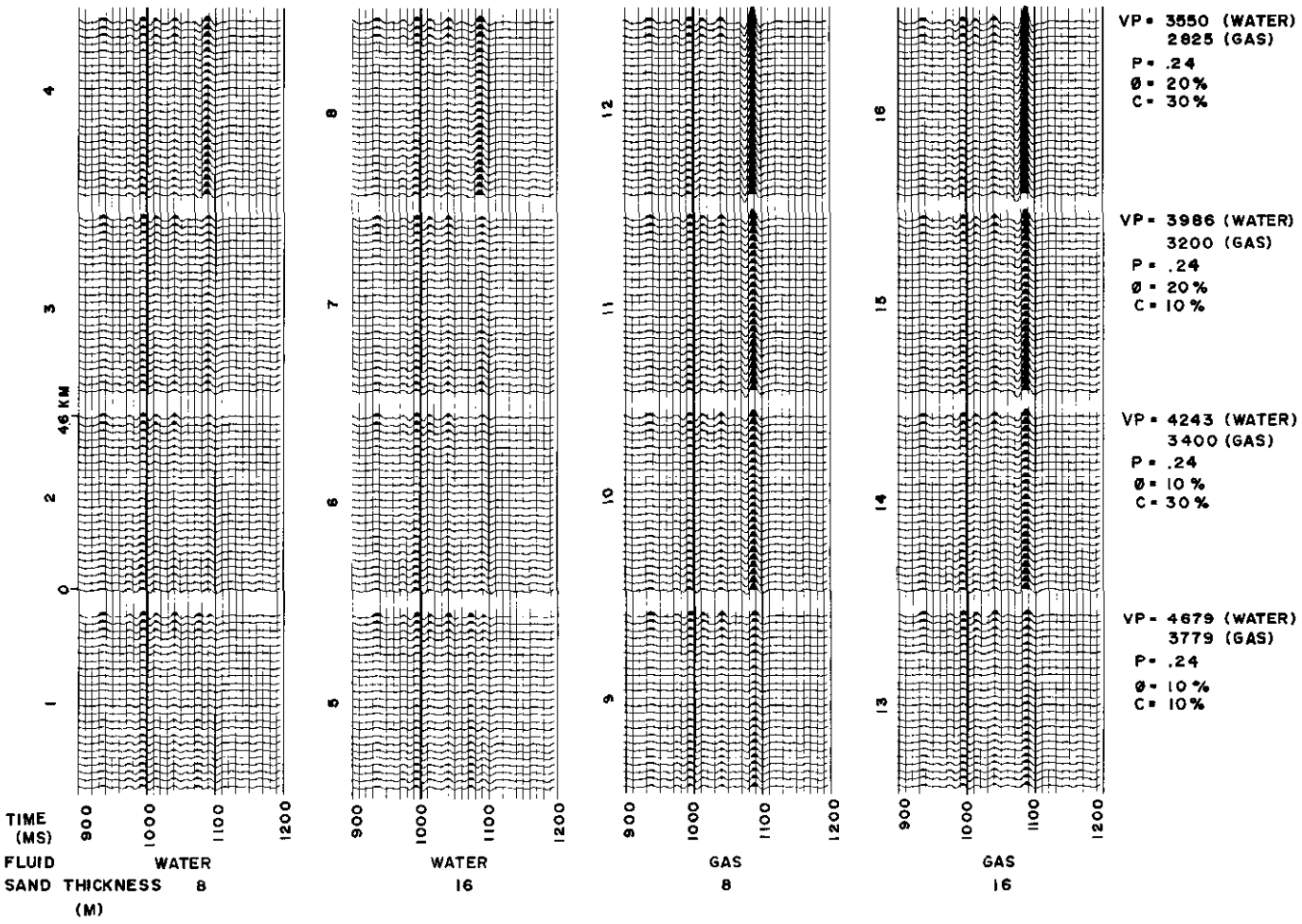

Fig. 11. Same synthetic as Figure 10 except that $P = 0.24$ for all models.

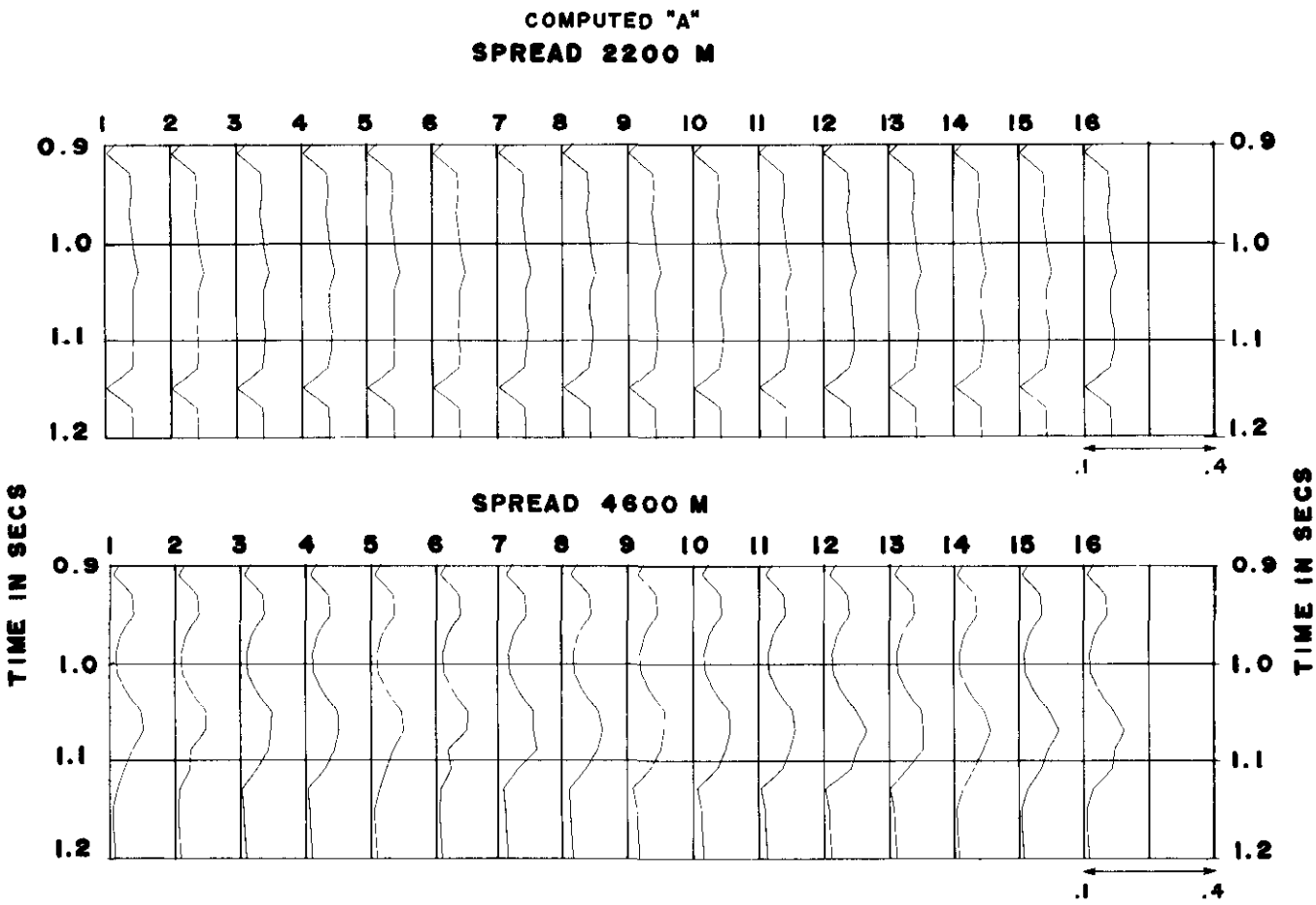

Fig. 12. Plot of *A* computed from an inversion of equation (1) and input data from the seismograms of Figure 10 using the same velocities used in generating the model. Trace numbers correspond to the model numbers in Figure 10.

References

Castagna, J.P., Batzle, M.L. and Eastwood, R.L., 1985, Relationships between compressional-wave and shear-wave velocities in clastic silicate rocks: Geophysics **50**, 571-581.

Domenico, S.N., 1974, Effect of water saturation on seismic reflectivity of sand reservoirs encased in shale: Geophysics **39**, 759-769.

_____, 1976, Effect of brine-gas mixture on velocity in an unconsolidated sand reservoir: Geophysics **41**, 882-894.

_____, 1984, Rock lithology and porosity determination from shear and compressional wave velocity: Geophysics **49**, 1188-1195.

Gardner, G.H.F., Gardner, L.W. and Gregory, A.R., 1974, Formation velocity and density — the diagnostic basics for stratigraphic traps: Geophysics **39**, 770-780.

Gregory, A.R., 1976, Fluid saturation effects on dynamic elastic properties of sedimentary rocks: Geophysics **41**, 895-921.

Han, D.H., Nur, A. and Morgan, D., 1986, Effects of porosity and clay content on wave velocities in sandstones: Geophysics **51**, 2093-2107.

Kuster, G.T. and Toksöz, M.N., 1974, Velocity and attenuation of seismic waves in two-phase media: Part I & II: Geophysics **39**, 587-618.

Ostrander, W.J., 1984, Plane-wave reflection coefficients for gas sands at non-normal angles of incidence: Geophysics **49**, 1637-1648.

Pickett, G.R., 1963, Acoustic character logs and their applications in formation evaluation: J. Can. Petr. Tech. **15**, 659-667.

Shuey, R.T., 1985, A simplification of the Zoeppritz equations: Geophysics **50**, 609-614.

Tatham, R.T., 1982, V_p/V_s and lithology: Geophysics **47**, 336-344.

Toksöz, M.N., Cheng, C.H. and Timur, A., 1976, Velocities of seismic waves in porous rocks: Geophysics **41**, 621-645.

Tooley, R.D., Spencer, T.W. and Sagoci, H.F., 1965, Reflection and transmission of plane compressional waves: Geophysics **30**, 552-570.

Varsek, J.L., Lausten, C.D., Blott, J.E. and Livingston, J.B., 1987, Seismic delineation of acoustically transparent reservoirs: A case history: Can. Soc. Expl. Geophys. Recorder **12**, 4, 6-14.

Wilkens, R., Simmons, G. and Carauso, L., 1984, The ratio V_p/V_s as a discriminant of composition of siliceous limestones: Geophysics **49**, 1850-1860.

Wren, A.E., 1984, Seismic techniques in Cardium exploration: J. Can. Soc. Expl. Geophys. **20**, 55-59.

Young, B.C. and Braile, L.W., 1976, A computer program for the application of Zoeppritz's amplitude equations and Knott's energy equation: Bull. Seis. Soc. Am. **66**, 1881-1885.